Resonant contribution of the three-body decay process $\bar{B}_s \to K^+K^-P$ in perturbative QCD*

Gang Lü (吕刚)[1†] Chang-Chang Zhang (张畅畅)[1‡] Yan-Lin Zhao (赵艳琳)[1§] Li-Ying Zhang (张丽英)[1¶]

[1]College of Science, Henan University of Technology, Zhengzhou 450001, China

Abstract: We investigate *CP* violation in the decay process $\bar{B}_s \to \phi(\rho,\omega)P \to K^+K^-P$ by considering the interference effects of $\phi \to K^+K^-$, $\rho \to K^+K^-$, and $\omega \to K^+K^-$within the framework of the perturbative QCD method (P refers to π, K, η, and η' pseudoscalar mesons). We analyze the mixings of $\phi-\rho^0$, $\phi-\omega$, and $\omega-\rho^0$ and provide the amplitudes of the quasi-two-body decay processes. The *CP* violation for the $\bar{B}_s \to K^+K^-P$ decay process is obvious in the ranges of the three vector meson interferences. Meanwhile, the localized *CP* violation can be found to compare with the experimental results from the three-body decay process at the LHC in the near future.

Keywords: heavy flavor physics, *CP* violation, *B* decay

DOI: 10.1088/1674-1137/ad0e03

I. INTRODUCTION

CP violation is a fascinating phenomenon in particle physics that has puzzled us for decades. The standard model (SM) of particle physics provides a framework for understanding *CP* violation; however, there are still many unanswered questions [1]. One area of research focuses on the search for new sources of *CP* violation beyond the Cabibbo-Kobayashi-Maskawa (CKM) matrix. This involves studying rare decays and interactions between particles to search for deviations from SM predictions. Another approach is to study *CP* violation in different types of particles, such as neutrinos and mesons. Despite these efforts, much remains unknown about *CP* violation.

In as early as 2012, the LHCb Collaboration confirmed the existence of *CP* violation in several three-body decay studies of *B* mesons and found that the local phase space of $\bar{B}^{\pm} \to \pi^+\pi^-\pi^{\pm}$ decay channels had large direct *CP* violation, which was an interesting phenomenon at the time [2, 3]. This phenomenon was later found to be explained by intermediate state resonances between different isospin mesons. The $\bar{B}^{\pm} \to \pi^+\pi^-\pi^{\pm}$ decay process was studied using $\rho-\omega$ mixed resonance and found significant *CP* violation in the invariant mass $m(\pi^+\pi^-) = 0.77$ GeV, which coincides with the position and degree of local *CP* violation [4]. There is no doubt that the three-body decay of heavy mesons is more complex than the two-body case, with one reason being that they receive both resonant and non-resonant contributions during the decay process. The existing experimental results show that *CP* asymmetry in some local regions of phase space may be more obvious. Similarly, the LHCb observed large asymmetries in local regions in $B^{\pm} \to K^{\pm}\pi^+\pi^-$ and $B^{\pm} \to K^{\pm}K^+K^-$. The invariant mass spectra of $B^{\pm} \to K^{\pm}\pi^+\pi^-$ decays in the region $0.08 < m^2_{\pi^+\pi^-} < 0.66\ \mathrm{GeV}^2/c^4$ and $m^2_{K^{\pm}\pi^{\mp}} < 15\ \mathrm{GeV}^2/c^4$, and $B^{\pm} \to K^{\pm}K^+K^-$ decays in the region $1.2 < m^2_{K^+K^-\mathrm{low}} < 2.0\ \mathrm{GeV}^2/c^4$ and $m^2_{K^+K^-\mathrm{high}} < 15\ \mathrm{GeV}^2/c^4$ [5]. These local apparent *CP* asymmetries are interesting. Currently, the phenomenon of *CP* asymmetry in the three-body decay process of B_s mesons remains relatively unexplored, with limited research from both theoretical and experimental perspectives.

This study aims to calculate the *CP* violation of the $\bar{B}_s \to K^+K^-P$ decay process via the perturbative QCD (PQCD) method because the Sudakov factor in PQCD effectively depresses the non-perturbative contribution and absorbs the non-perturbative part into the universal hadronic wave function [6]. Moreover, this method is self-consistent in the two-body non-leptonic decay process of *B* mesons and has been proved to exhibit the large *CP* vi-

Received 29 October 2023; Accepted 20 November 2023; Published online 21 November 2023

* Supported by the Natural Science Foundation of Henan Province, China (232300420115).

† E-mail: ganglv66@sina.com

‡ E-mail: 1219765284@qq.com

§ E-mail: zyl163mail@163.com

¶ E-mail: zhangly0324@163.com

olation found in experiments [7]. Indeed, the corresponding two-body decay process of the B meson has been well-established and developed into various three-body decay processes, and we can treat three-body decay processes using the method of quasi-two body decay processes [8, 9]. In recent years, an increasing number of analyses on precious measurements of branching ratios and CP violation in three-body decay processes have been performed by BaBar [10], Belle II [11], CLEO [12], and LHCb, which provides a great platform to test the SM and search new physical signals. In this study, we take the method of quasi-two-body decay processes to calculate the CP violation of the $\bar{B}_s \to K^+K^-P$ process under the mixing mechanism of $\phi \to K^+K^-$, $\rho^0 \to K^+K^-$, and $\omega \to K^+K^-$.

The motivation for investigating the resonance effect among three particles originates from the adjacent masses of $\phi(1020)$, $\omega(782)$, and $\rho^0(770)$. The hybrid mechanism, primarily rooted in the vector meson dominance (VMD) model, is founded on vector mesons. This process involves the integration of vector meson contributions within the photon propagator in vacuum, where vector mesons are regarded as propagators interacting with photons. The fundamental postulate of this model posits that vector mesons are the primary constituents, suggesting that the hadronic element of photon vacuum polarization precisely constitutes a vector meson that is bound by quark-antiquark pairs [13, 14]. By incorporating information on K^+K^- production and considering the constraints imposed by isospin symmetry, the quark model, and the OZI rule, it becomes feasible to disentangle amplitudes with isospin $I = 1$ and $I = 0$ components. $\phi(1020)$ and $\omega(782)$ match the isospin $I = 0$ component. The $I = 1$ component derives from $\rho^0(770)$. In this study, the ideal field of intermediate states is transformed into a computable physical field through the application of a unitary matrix. Additionally, we investigate localized CP violation within the hybrid resonance range to facilitate meaningful future comparisons with experimental results.

We present our work in six parts. The mechanism of three vector meson mixing is introduced in Section II. In Section III, we initially investigate CP violation arising from the involvement of the mixing mechanism in the decay process $\bar{B}_s \to \phi(\rho^0,\omega)P \to K^+K^-P$. Subsequently, we present a formalism for local CP violation. In Section IV, we introduce the amplitude formalism within the framework of the PQCD method, along with the fundamental functions and associated parameters. Additionally, we provide an evaluation of both the magnitude and integrated form of CP violation. An analysis of the data results can be found in Section V. Finally, we engage in a comprehensive discussion and provide a concise summary of our findings.

II. MECHANISM OF THREE VECTOR MESON MIXING

Positive and negative electrons annihilate into photons and then are polarized in a vacuum to form the mesons $\phi(1020)$, $\rho^0(770)$, and $\omega(782)$, which can also decay into a K^+K^- pair. Meanwhile, the momentum can also be passed through the VMD model [15, 16]. Because the intermediate state particle is an un-physical state, we must convert it into a physical field from an isospin field through the matrix R [17]. Then, we can obtain the physical states of ϕ, ρ^0, and ω. Note that there is no $\phi-\rho^0-\omega$ mixing in the physical state, and we neglect the contribution of the high-order term [18]. The physical states $\phi-\rho^0-\omega$ can be expressed as linear combinations of the isospin states $\phi_I-\rho_I^0-\omega_I$. This relationship can be represented by the following matrix:

$$\begin{pmatrix} \rho^0 \\ \omega \\ \phi \end{pmatrix} = R(s) \begin{pmatrix} \rho_I^0 \\ \omega_I \\ \phi_I \end{pmatrix}, \tag{1}$$

where

$$R = \begin{pmatrix} \langle \rho_I|\rho\rangle & \langle \omega_I|\rho\rangle & \langle \phi_I|\rho\rangle \\ \langle \rho_I|\omega\rangle & \langle \omega_I|\omega\rangle & \langle \phi_I|\omega\rangle \\ \langle \rho_I|\phi\rangle & \langle \omega_I|\phi\rangle & \langle \phi_I|\phi\rangle \end{pmatrix}. \tag{2}$$

The change between the physical and isospin fields in the intermediate state of the decay process is related by the matrix R. The off-diagonal elements of R present information on $\phi-\rho^0-\omega$ mixing. Based on the isospin representation of ϕ_I, ρ_I, and ω_I, the isospin vector $|I,I_3\rangle$ can be constructed, where I_3 denotes the third component of isospin. The variables i and j are used to denote the physical state of the particle and the isospin basis vector, respectively. According to the orthogonal normalization relationship, we can derive the following: $\sum_j |j\rangle\langle j| = \sum_{j_I} |j_I\rangle\langle j_I| = I$, and $\langle j|i\rangle = \langle j_I|i_I\rangle = \delta_{ji}$. We use the notation $F_{V_iV_j}$ to denote the mixing parameter, where V_i and V_j represent one of the three vector particles. Then, the transformation matrix R can be converted as follows:

$$R = \begin{pmatrix} 1 & -F_{\rho\omega}(s) & -F_{\rho\phi}(s) \\ F_{\rho\omega}(s) & 1 & -F_{\omega\phi}(s) \\ F_{\rho\phi}(s) & F_{\omega\phi}(s) & 1 \end{pmatrix}. \tag{3}$$

From the translation of the two representations, the physical states can be written as

$$\begin{aligned}\phi &= F_{\rho\phi}(s)\rho_I^0 + F_{\omega\phi}(s)\omega_I + \phi_I,\\ \omega &= F_{\rho\omega}(s)\rho_I^0 + \omega_I - F_{\omega\phi}(s)\phi_I,\\ \rho^0 &= \rho_I^0 - F_{\rho\omega}(s)\omega_I - F_{\rho\phi}(s)\phi_I.\end{aligned} \tag{4}$$

The relationship between the mixing parameters $\Pi_{V_iV_j}$ and $F_{V_iV_j}$ can be deduced from the equations

$$\begin{aligned}F_{\rho\omega} &= \frac{\Pi_{\rho\omega}}{s_\rho - s_\omega},\\ F_{\rho\phi} &= \frac{\Pi_{\rho\phi}}{s_\rho - s_\phi},\\ F_{\omega\phi} &= \frac{\Pi_{\omega\phi}}{s_\omega - s_\phi}.\end{aligned} \tag{5}$$

The relationship $F_{V_iV_j} = -F_{V_jV_{V_i}}$ can be found. The inverse propagator of the vector meson, denoted as s_V ($V = \phi, \rho$, or ω), is defined such that $s_V = s - m_V^2 + \mathrm{i}m_V\Gamma_V$. The variables m_V and Γ_V represent the mass and decay rate of the vector mesons, respectively. Meanwhile, $\sqrt{s}$ denotes the invariant mass of the K^+K^- pairs.

In this study, the momentum dependence of the mixing parameters $\Pi_{V_iV_j}$ of V_iV_j mixing is introduced to obtain the obvious s dependence. The mixing parameter $\Pi_{\rho\omega} = -4470 \pm 250 \pm 160 - \mathrm{i}(5800 \pm 2000 \pm 1100)\mathrm{MeV}^2$ is obtained near the ρ meson, as recently determined precisely by Wolfe and Maltnan [19–21]. The mixing parameter $\Pi_{\omega\phi} = 19000 + \mathrm{i}(2500 \pm 300)\mathrm{MeV}^2$ is obtained near the ϕ muon, and the mixing parameter $\Pi_{\phi\rho} = 720 \pm 180 - \mathrm{i}(870 \pm 320)\mathrm{MeV}^2$ is obtained near the ϕ meson [22]. Then, we define

$$\widetilde{\Pi}_{\rho\omega} = \frac{s_\rho\Pi_{\rho\omega}}{s_\rho - s_\omega},\ \widetilde{\Pi}_{\rho\phi} = \frac{s_\rho\Pi_{\rho\phi}}{s_\rho - s_\phi},\ \widetilde{\Pi}_{\phi\omega} = \frac{s_\phi\Pi_{\phi\omega}}{s_\phi - s_\omega}. \tag{6}$$

III. *CP* VIOLATION IN THE $\bar{B}_s \to \phi\,(\rho^0, \omega)$ $P \to K^+K^-P$ DECAY PROCESS

A. Resonance effect from $V \to K^+K^-$

We present decay diagrams (a)-(i) of the $\bar{B}_s \to \phi(\rho^0, \omega)P \to K^+K^-P$ process in Fig. 1, aiming to provide a more comprehensive understanding of the mixing mechanism.

In the above decay diagrams, the decay processes depicted in (a), (d), and (g) represent direct decay modes, where K^+K^- are produced through ϕ, ρ^0, and ω, respectively. The quasi-two-body approach employed in this study is evident from the aforementioned diagrams. Compared to the direct decay processes depicted in diagrams (a), (d), and (g) of Fig. 1, the K^+K^- pair can also be generated through a distinct mixing mechanism. The black dots in the figure represent the resonance effect between these two mesons, denoted by the mixing parameter $\Pi_{V_iV_j}$. Although the contribution from this mixing mechanism is relatively small compared to other diagrams in Fig. 1, it must be considered.

The amplitude of the $\bar{B}_s \to \phi\,(\rho^0, \omega)\ P \to K^+K^-P$ decay channel can be characterized in the following manner:

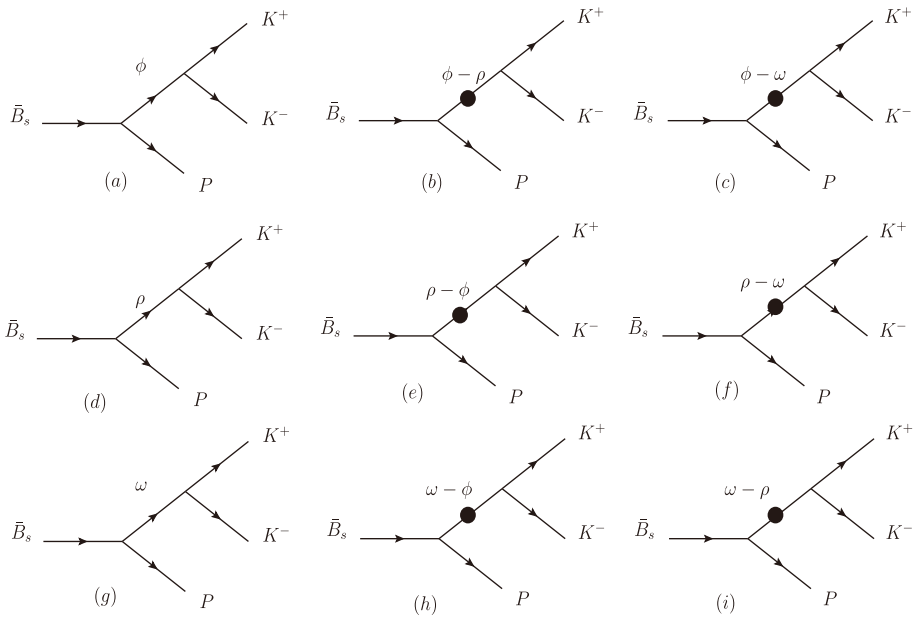

Fig. 1. Decay diagrams of the $\bar{B}_s \to \phi(\rho^0, \omega)P \to K^+K^-P$ process.

$$A = \left\langle K^+K^-P\left|H^T\right|\bar{B}_s\right\rangle + \left\langle K^+K^-P\left|H^P\right|\bar{B}_s\right\rangle, \quad (7)$$

where the quantities $\left\langle K^+K^-P\left|H^P\right|\bar{B}_s\right\rangle$ and $\left\langle K^+K^-P\left|H^T\right|\bar{B}_s\right\rangle$ represent the amplitudes associated with penguin-level and tree-level contributions, respectively. The propagator of the intermediate vector meson can be transformed from the diagonal matrix to the physical state after applying the R matrix transformation. Neglecting higher order terms, the amplitudes can be as demonstrated as

$$\begin{aligned}\left\langle K^+K^-P\left|H^T\right|\bar{B}_s\right\rangle =& \frac{g_\phi}{s_\phi}t_\phi + \frac{g_\rho}{s_\rho s_\phi}\widetilde{\Pi}_{\rho\phi}t_\phi + \frac{g_\omega}{s_\omega s_\phi}\widetilde{\Pi}_{\omega\phi}t_\phi \\ &+ \frac{g_\rho}{s_\rho}t_\rho + \frac{g_\phi}{s_\phi s_\rho}\widetilde{\Pi}_{\phi\rho}t_\rho + \frac{g_\omega}{s_\omega s_\rho}\widetilde{\Pi}_{\omega\rho}t_\rho \\ &+ \frac{g_\omega}{s_\omega}t_\omega + \frac{g_\phi}{s_\phi s_\omega}\widetilde{\Pi}_{\phi\omega}t_\omega + \frac{g_\rho}{s_\rho s_\omega}\widetilde{\Pi}_{\rho\omega}t_\omega, \quad (8)\end{aligned}$$

$$\begin{aligned}\left\langle K^+K^-P\left|H^P\right|\bar{B}_s\right\rangle =& \frac{g_\phi}{s_\phi}p_\phi + \frac{g_\rho}{s_\rho s_\phi}\widetilde{\Pi}_{\rho\phi}p_\phi + \frac{g_\omega}{s_\omega s_\phi}\widetilde{\Pi}_{\omega\phi}p_\phi \\ &+ \frac{g_\rho}{s_\rho}p_\rho + \frac{g_\phi}{s_\phi s_\rho}\widetilde{\Pi}_{\phi\rho}p_\rho + \frac{g_\omega}{s_{\omega s_\rho}}\widetilde{\Pi}_{\omega\rho}p_\rho \\ &+ \frac{g_\omega}{s_\omega}p_\omega + \frac{g_\phi}{s_\phi s_\omega}\widetilde{\Pi}_{\phi\omega}p_\omega + \frac{g_\rho}{s_\rho s_\omega}\widetilde{\Pi}_{\rho\omega}p_\omega, \quad (9)\end{aligned}$$

where the tree-level (penguin-level) amplitudes $t_\rho\left(p_\rho\right)$, $t_\omega(p_\omega)$, and $t_\phi\left(p_\phi\right)$ correspond to the decay processes $\bar{B}_s \to \rho^0 P$, $\bar{B}_s \to \omega P$, and $\bar{B}_s \to \phi P$, respectively. Here, s_V represents the inverse propagator of the vector meson V [23]. Moreover, g_V represents the coupling constant derived from the decay process of $V \to K^+K^-$ and can be expressed as $\sqrt{2}g_{\rho k^+k^-} = \sqrt{2}g_{\omega k^+k^-} = -g_{\phi k^+k^-} = 4.54$ [24].

The differential parameter for CP asymmetry can be expressed as follows:

$$A_{CP} = \frac{|A|^2 - \left|\overline{A}\right|^2}{|A|^2 + \left|\overline{A}\right|^2}. \quad (10)$$

B. Localized *CP* violation of A_{CP}^{Ω}

In this study, we perform the integral calculation of A_{CP} to facilitate future experimental comparisons. For the decay process $\bar{B}_s \to \phi P$, the amplitude is given by $M^{\lambda}_{\bar{B}_s\to\phi P} = \alpha p_{\bar{B}}\cdot\epsilon^*(\lambda)$, where $p_{\bar{B}_s}$ represents the momenta of the $\bar{B}_s$ meson, ϵ denotes the polarization vector of ϕ, and λ corresponds to its polarization. The parameter α remains independent of λ. Similarly, in the decay process $\phi \to K^+K^-$, we can express $M^{\lambda}_{\phi\to K^-K^+} = g_\phi\epsilon(\lambda)(p_1 - p_2)$, where p_1 and p_2 denote the momenta of the produced K^+ and K^- particles from ϕ, respectively. Here, the parameter g_ϕ represents an effective coupling constant for $\phi \to K^+K^-$. Regarding the dynamics of meson decay, the polarization vector of a vector meson satisfies $\sum_{\lambda=0,\pm1}\epsilon^{\lambda}_{\mu}(p)(\epsilon^{\lambda}_{\nu}(p))^* = -(g_{\mu\nu} - p_\mu p_\nu/m_V^2)$. As a result, we obtain the total amplitude for the decay process $\bar{B}_s \to \phi P \to K^+K^-P$ [4, 25, 26]:

$$\begin{aligned}A =& \alpha p^{\mu}_{\bar{B}_s}\frac{\sum_\lambda \epsilon^*_\mu(\lambda)\epsilon_\nu(\lambda)}{s_\phi}g_{\phi kk}(p_1 - p_2)^\nu \\ =& \frac{g_{\phi kk}\alpha}{s_\phi}\cdot p^{\mu}_{\bar{B}_s}\left[g_{\mu\nu} - \frac{(p_1+p_2)_\mu(p_1+p_2)_\nu}{s}\right](p_1 - p_2)^\nu \\ =& \frac{g_{\phi kk}}{s_\phi}\cdot\frac{M^{\lambda}_{\bar{B}_s\to\phi\pi^0}}{p_{\bar{B}_s}\cdot\epsilon^*}\cdot\left(\Sigma - s'\right) \\ =& \left(\Sigma - s'\right)\cdot\mathcal{A}.\end{aligned} \quad (11)$$

The high $(\sqrt{s'})$ and low $\sqrt{s}$ ranges are defined to calculate the invariant mass of K^-K^+. By setting a fixed value for s, we can determine an appropriate value for s' that fulfills the equation $\Sigma = \left(s'_{\max} + s'_{\min}\right)/2$, where $s'_{\max}(s'_{\min})$ denotes the maximum (minimum) value.

Utilizing the principles of three-body kinematics, we can deduce the local CP asymmetry for the decay $\bar{B}_s \to K^+K^-P$ within a specific range of invariant mass:

$$A^{\Omega}_{CP} = \frac{\int_{s_1}^{s_2}\mathrm{d}s\int_{s'_1}^{s'_2}\mathrm{d}s'(\Sigma - s')^2\left(|\mathcal{A}|^2 - |\overline{\mathcal{A}}|^2\right)}{\int_{s_1}^{s_2}\mathrm{d}s\int_{s'_1}^{s'_2}\mathrm{d}s'(\Sigma - s')^2\left(|\mathcal{A}|^2 + |\overline{\mathcal{A}}|^2\right)}. \quad (12)$$

Our calculation considers the dependence of $\Sigma = \left(s'_{\max} + s'_{\min}\right)/2$ on s', assuming that $s'_{\max} > s' > s'_{\min}$ represents an integral interval of high invariant mass for the K^-K^+ meson pair, and $\int_{s'_1}^{s'_2}\mathrm{d}s'(\Sigma - s')^2$ represents a factor dependent on s'. The correlation between Σ and s' can be easily determined through kinematic analysis because s' only varies on a small scale. Therefore, we can consider Σ as a constant. This allows us to cancel out the term $\int_{s'_1}^{s'_2}\mathrm{d}s'(\Sigma - s')^2$ in both the numerator and denominator, resulting in A^{Ω}_{CP} no longer depending on the high invariant mass of positive and negative particles.

IV. AMPLITUDES OF QUASI-TWO-BODY DECAY PROCESSES WITHIN THE FRAMEWORK OF PERTURBATIVE QCD

A. Formulation of calculations

The three-body decay process is accompanied by intricate and multifaceted dynamical mechanisms. The PQCD method is known for its efficacy in handling perturbation corrections. It has been successfully applied to two-body non-light decay processes and also exhibits

promise for quasi-two-body decay processes. In the framework of PQCD, within the rest frame of a heavy B meson, the decay process involves the production of two light mesons with significantly large momenta that exhibit rapid motion. The dominance of hard interactions in this decay amplitude arises owing to insufficient time to exchange soft gluons with final-state mesons. Given the high velocity of these final-state mesons, a hard gluon imparts momentum to the light spectator quark within the B meson, resulting in the formation of a rapidly moving final-state meson. Consequently, this hard interaction is described by six quark operators. The nonperturbative dynamics are encapsulated within the meson wave function, which can be extracted through experimental measurements. However, employing perturbation theory allows for the computation of this hard contribution. Quasi-two-body decay can be computed by defining the intermediate state of decay.

Using the quasi-two-body decay method, the total amplitude of $\bar{B}_s \to \phi\ (\rho^0,\ \omega)\ \pi^0 \to K^+K^-\pi^0$ is composed of two components: $\bar{B}_s \to \phi\ (\rho^0,\ \omega)\ \pi^0$ and $\phi\ (\rho^0,\ \omega) \to K^+K^-$. In this study, we illustrate the methodology of the quasi-two-body decay process using the example of $\bar{B}_s \to \phi\pi^0 \to K^+K^-\pi^0$, based on matrix elements involving V_{tb}, V_{ts}^*, and V_{ub}, V_{ub}^*.

$$\begin{aligned}\sqrt{2}A\left(\bar{B}_s \to \pi^0\phi\left(\phi \to K^+K^-\right)\right) =& \frac{G_F p_{\bar{B}_s}\cdot\sum_{\lambda=0,\pm1}\epsilon(\lambda)g_\phi\epsilon^*(\lambda)\cdot(p_{k^+}-p_{k^-})}{\sqrt{2}s_\phi}\\ &\times\left\{V_{ub}V_{us}^*\left[f_\pi F^{LL}_{\bar{B}_s\to\phi}(a_2)+M^{LL}_{\bar{B}_s\to\phi}(C_2)\right]\right.\\ &\left.-V_{tb}V_{ts}^*\left[f_\pi F^{LL}_{\bar{B}_s\to\phi}\left(\frac{3}{2}a_9-\frac{3}{2}a_7\right)+M^{LL}_{\bar{B}_s\to\phi}\left(\frac{3}{2}C_8+\frac{3}{2}C_{10}\right)\right]\right\},\end{aligned} \tag{13}$$

where $P_{\bar{B}_s}$, p_{k^+}, and p_{k^-} are the momenta of $\bar{B}_s$, K^+, and K^-, respectively, C_i (a_i) is the Wilson coefficient (associated Wilson coefficient), ϵ is the polarization of the vector meson, G_F is the Fermi constant, and f_π refers to the decay constants of π [27]. Furthermore, $F^{LL}_{\bar{B}_s\to\phi}$ and $M^{LL}_{\bar{B}_s\to\phi}$ represent emission graphs that are factorable and non-factorable, respectively, and F^{LL}_{ann} and M^{LL}_{ann} represent annihilation graphs that are factorable and non-factorable, respectively. LL, LR, and SP correspond to three flow structures [6].

The additional representations of the three-body decay amplitudes that should be considered to calculate CP violation through the mixed mechanism in this study are as follows:

$$\begin{aligned}2A\left(\bar{B}_s^0 \to \rho^0\left(\rho^0 \to K^+K^-\right)\pi^0\right) =& \frac{G_F p_{\bar{B}_s^0}\cdot\sum_{\lambda=0,\pm1}\epsilon(\lambda)g_\rho\epsilon^*(\lambda)\cdot(p_{k^+}-p_{k^-})}{\sqrt{2}s_\rho}\\ &\times\left\{V_{ub}V_{us}^*\left[f_{B_s}F^{LL}_{ann}(a_2)+M^{LL}_{ann}(C_2)+f_{B_s}F^{LL'}_{ann}(a_2)+M^{LL'}_{ann}(C_2)\right]\right.\\ &-V_{tb}V_{ts}^*\left[f_{B_s}F^{LL}_{ann}(a_3+a_9)\ -f_{B_s}F^{LR}_{ann}(a_5+a_7)+M^{LL}_{ann}(C_4+C_{10})\right.\\ &-M^{SP}_{ann}(C_6+C_8)+\left[\pi^+\leftrightarrow\rho^-\right]+f_{B_s}F^{LL'}_{ann}(a_3+a_9)-f_{B_s}F^{LR'}_{ann}(a_5+a_7)\\ &\left.\left.+M^{LL'}_{ann}(C_4+C_{10})-M^{SP'}_{ann}(C_6+C_8)+\left[\rho^+\leftrightarrow\pi^-\right]\right]\right\}.\end{aligned} \tag{14}$$

$$\begin{aligned}2A\left(\bar{B}_s^0 \to \pi^0\omega\left(\omega \to K^+K^-\right)\right) =& \frac{G_F p_{\bar{B}_s^0}\cdot\sum_{\lambda=0,\pm1}\epsilon(\lambda)g_\omega\epsilon^*(\lambda)\cdot(p_{k^+}-p_{k^-})}{\sqrt{2}s_\omega}\\ &\times\left\{V_{ub}V_{us}^*M^{LL}_{ann}(c_2)-V_{tb}V_{ts}^*\left[M^{LL}_{ann}\left(\frac{3}{2}c_{10}\right)-M^{SP}_{ann}\left(\frac{3}{2}c_8\right)+\left[\pi^0\leftrightarrow\omega\right]\right]\right\}.\end{aligned} \tag{15}$$

$$\begin{aligned}A\left(\bar{B}_s^0 \to K^0\phi\left(\phi \to K^+K^-\right)\right) =& \frac{G_F p_{\bar{B}_s^0}\cdot\sum_{\lambda=0,\pm1}\epsilon(\lambda)g_\phi\epsilon^*(\lambda)\cdot(p_{k^+}-p_{k^-})}{\sqrt{2}s_\phi}\\ &\times\left\{-V_{tb}V_{td}^*\left[f_\phi F^{LL}_{B_s\to K}\left(a_3+a_5-\frac{1}{2}a_7-\frac{1}{2}a_9\right)+f_K F^{LL}_{B_s\to\phi}\left(a_4-\frac{1}{2}a_{10}\right)\right.\right.\end{aligned}$$

$$
\begin{aligned}
&-f_K F^{SP}_{B_s\to\phi}\left(a_6-\frac{1}{2}a_8\right)+M^{LL}_{B_s\to K}\left(C_4-\frac{1}{2}C_{10}\right)+M^{LL}_{B_s\to\phi}\left(C_3-\frac{1}{2}C_9\right)\\
&-M^{SP}_{B_s\to K}\left(C_6-\frac{1}{2}C_8\right)-M^{LR}_{B_s\to\phi}\left(C_5-\frac{1}{2}C_7\right)+f_{B_s}F^{LL}_{ann}\left(a_4-\frac{1}{2}a_{10}\right)\\
&-f_{B_s}F^{SP}_{ann}\left(a_6-\frac{1}{2}a_8\right)+M^{LL}_{ann}\left(C_3-\frac{1}{2}C_9\right)-M^{LR}_{ann}\left(C_5-\frac{1}{2}C_7\right)\Big]\Big\}. \qquad (16)
\end{aligned}
$$

$$
\begin{aligned}
\sqrt{2}A\left(\bar{B}^0_s\to K^0\rho\left(\rho\to K^+K^-\right)\right)=&\frac{G_F p_{\bar{B}^0_s}\cdot\sum_{\lambda=0,\pm1}\epsilon(\lambda)g_\phi\epsilon^*(\lambda)\cdot(p_{k^+}-p_{k^-})}{\sqrt{2}s_\rho}\\
&\times\Big\{V_{ub}V^*_{ud}\left[f_\rho F^{LL}_{B_s\to K}(a_2)+M^{LL}_{B_s\to K}(C_2)\right]-V_{tb}V^*_{td}\Big[M^{LR}_{B_s\to K}\left(-C_5+\frac{1}{2}C_7\right)\\
&+f_\rho F^{LL}_{B_s\to K}\left(-a_4+\frac{3}{2}a_7+\frac{1}{2}a_{10}+\frac{3}{2}a_9\right)-M^{SP}_{B_s\to K}\left(\frac{3}{2}C_8\right)\\
&+M^{LL}_{B_s\to K}\left(-C_3+\frac{1}{2}C_9+\frac{3}{2}C_{10}\right)+f_{B_s}F^{LL}_{ann}\left(-a_4+\frac{1}{2}a_{10}\right)\\
&+f_{B_s}F^{SP}_{ann}\left(-a_6+\frac{1}{2}a_8\right)+M^{LL}_{ann}\left(-C_3+\frac{1}{2}C_9\right)+M^{LR}_{ann}\left(-C_5+\frac{1}{2}C_7\right)\Big]\Big\}. \qquad (17)
\end{aligned}
$$

$$
\begin{aligned}
\sqrt{2}A\left(\bar{B}^0_s\to K^0\omega\left(\omega\to K^+K^-\right)\right)=&\frac{G_F p_{\bar{B}^0_s}\cdot\sum_{\lambda=0,\pm1}\epsilon(\lambda)g_\omega\epsilon^*(\lambda)\cdot(p_{k^+}-p_{k^-})}{\sqrt{2}s_\omega}\\
&\times\Big\{V_{ub}V^*_{ud}\left[f_\omega F^{LL}_{B_s\to K}(a_2)+M^{LL}_{B_s\to K}(C_2)\right]-V_{tb}V^*_{td}\Big[M^{LR}_{B_s\to K}\left(C_5-\frac{1}{2}C_7\right)\\
&+f_\omega F^{LL}_{B_s\to K}\left(2a_3+a_4+2a_5+\frac{1}{2}a_7+\frac{1}{2}a_9-\frac{1}{2}a_{10}\right)\\
&+M^{LL}_{B_s\to K}\left(C_3+2C_4-\frac{1}{2}C_9+\frac{1}{2}C_{10}\right)+M^{LL}_{ann}\left(C_3-\frac{1}{2}C_9\right)\\
&-M^{SP}_{B_s\to K}\left(2C_6+\frac{1}{2}C_8\right)+f_{B_s}F^{LL}_{ann}\left(a_4-\frac{1}{2}a_{10}\right)\\
&+f_{B_s}F^{SP}_{ann}\left(a_6-\frac{1}{2}a_8\right)+M^{LR}_{ann}\left(C_5-\frac{1}{2}C_7\right)\Big]\Big\}. \qquad (18)
\end{aligned}
$$

$$
\begin{aligned}
A\left(\bar{B}^0_s\to\eta\phi\left(\phi\to K^+K^-\right)\right)=&\frac{G_F p_{\bar{B}^0_s}\cdot\sum_{\lambda=0,\pm1}\epsilon(\lambda)g_\phi\epsilon^*(\lambda)\cdot(p_{k^+}-p_{k^-})}{\sqrt{2}s_\phi}\times\Big\{\frac{\cos\theta}{\sqrt{2}}\Big\{V_{ub}V^*_{us}\left[f_n F^{LL}_{B_s\to\phi}(a_2)+M^{LL}_{B_s\to\phi}(C_2)\right]\\
&-V_{tb}V^*_{ts}\Big[f_n F^{LL}_{B_s\to\phi}\left(2a_3-2a_5-\frac{1}{2}a_7+\frac{1}{2}a_9\right)\\
&+M^{LL}_{B_s\to\phi}\left(2C_4+\frac{1}{2}C_{10}\right)+M^{SP}_{B_s\to\phi}\left(2C_6+\frac{1}{2}C_8\right)\Big]\Big\}\\
&-\sin\theta\Big\{-V_{tb}V^*_{ts}\Big[f_s F^{LL'}_{B_s\to\phi}\left(a_3+a_4-a_5+\frac{1}{2}a_7-\frac{1}{2}a_9-\frac{1}{2}a_{10}\right)\\
&+M^{SP'}_{B_s\to\phi}\left(C_6-\frac{1}{2}C_8\right)+f_{B_s}F^{LL'}_{ann}\left(a_3+a_4-a_5+\frac{1}{2}a_7-\frac{1}{2}a_9-\frac{1}{2}a_{10}\right)\\
&+M^{LL'}_{ann}\left(C_3+C_4-\frac{1}{2}C_9-\frac{1}{2}C_{10}\right)-f_{B_s}F^{SP'}_{ann}\left(a_6-\frac{1}{2}a_8\right)\\
&-M^{LR'}_{ann}\left(C_5-\frac{1}{2}C_7\right)-M^{SP'}_{ann}\left(C_6-\frac{1}{2}C_8\right)\Big]+\left[\eta_s\leftrightarrow\phi\right]\Big\}\Big\}. \qquad (19)
\end{aligned}
$$

$$
\begin{aligned}
A\left(\bar{B}_s^0 \to \eta\rho^0\left(\rho^0 \to K^+K^-\right)\right) =& \frac{G_F p_{\bar{B}_s^0}\cdot\sum_{\lambda=0,\pm1}\epsilon(\lambda)g_\rho\epsilon^*(\lambda)\cdot(p_{k^+}-p_{k^-})}{\sqrt{2}s_\rho} \\
&\times\left\{\frac{\cos\theta}{2}\left\{-V_{tb}V_{ts}^*\left[f_{B_s}F_{ann}^{LL}\left(\frac{3}{2}a_9-\frac{3}{2}a_7\right)+M_{ann}^{LL}\left(\frac{3}{2}C_{10}\right)-M_{ann}^{SP}\left(\frac{3}{2}C_8\right)\right]\right.\right. \\
&\left.+V_{ub}V_{us}^*\left[f_{B_s}F_{ann}^{LL}(a_2)+M_{ann}^{LL}(C_2)\right]+\left[\rho^0\leftrightarrow\eta_n\right]\right\} \\
&-\frac{\sin\theta}{\sqrt{2}}\left\{V_{ub}V_{us}^*\left[f_\rho F_{B_s\to\eta_s}^{LL'}(a_2)+M_{B_s\to\eta_s}^{LL'}(C_2)\right]\right. \\
&\left.\left.-V_{tb}V_{ts}^*\left[f_\rho F_{B_s\to\eta_s}^{LL'}\left(\frac{3}{2}a_7+\frac{3}{2}a_9\right)+M_{B_s\to\eta_s}^{LL'}\left(\frac{3}{2}C_{10}\right)-M_{B_s\to\eta_s}^{SP'}\left(\frac{3}{2}C_8\right)\right]\right\}\right\}. \qquad (20)
\end{aligned}
$$

$$
\begin{aligned}
A\left(\bar{B}_s^0 \to \eta\omega\left(\omega \to K^+K^-\right)\right) =& \frac{G_F p_{\bar{B}_s^0}\cdot\sum_{\lambda=0,\pm1}\epsilon(\lambda)g_\omega\epsilon^*(\lambda)\cdot(p_{k^+}-p_{k^-})}{\sqrt{2}s_\omega} \\
&\times\left\{\frac{\cos\theta}{2}\left\{V_{ub}V_{us}^*\left[f_{B_s}F_{ann}^{LL}(a_2)+M_{ann}^{LL}(C_2)\right]\right.\right. \\
&-V_{tb}V_{ts}^*\left[M_{ann}^{LL}\left(2C_4+\frac{1}{2}C_{10}\right)-M_{ann}^{SP}\left(2C_6+\frac{1}{2}C_8\right)\right. \\
&\left.\left.+\ f_{B_s}F_{ann}^{LL}\left(2a_3-2a_5-\frac{1}{2}a_7+\frac{1}{2}a_9\right)\right]+\left[\eta_n\leftrightarrow\omega\right]\right\} \\
&-\frac{\sin\theta}{\sqrt{2}}\left\{V_{ub}V_{us}^*\left[f_\omega F_{B_s\to\eta_s}^{LL'}(a_2)+M_{B_s\to\eta_s}^{LL'}(C_2)\right]\right. \\
&-V_{tb}V_{ts}^*\left[f_\omega F_{B_s\to\eta_s}^{LL'}\left(2a_3+2a_5+\frac{1}{2}a_7+\frac{1}{2}a_9\right)\right. \\
&\left.\left.+M_{B_s\to\eta_s}^{LL'}\left(2C_4+\frac{1}{2}C_{10}\right)-M_{B_s\to\eta_s}^{SP'}\left(2C_6+\frac{1}{2}C_8\right)\right]\right\}\right\}. \qquad (21)
\end{aligned}
$$

$$
\begin{aligned}
A\left(\bar{B}_s^0 \to \eta'\phi\left(\phi \to K^+K^-\right)\right) =& \frac{G_F p_{\bar{B}_s^0}\cdot\sum_{\lambda=0,\pm1}\epsilon(\lambda)g_\phi\epsilon^*(\lambda)\cdot(p_{k^+}-p_{k^-})}{\sqrt{2}s_\phi} \\
&\times\left\{\frac{\sin\theta}{\sqrt{2}}\left\{V_{ub}V_{us}^*\left[f_n F_{B_s\to\phi}^{LL}(a_2)+M_{B_s\to\phi}^{LL}(C_2)\right]\right.\right. \\
&-V_{tb}V_{ts}^*\left[f_n F_{B_s\to\phi}^{LL}\left(2a_3-2a_5-\frac{1}{2}a_7+\frac{1}{2}a_9\right)\right. \\
&\left.\left.+M_{B_s\to\phi}^{LL}\left(2C_4+\frac{1}{2}C_{10}\right)+M_{B_s\to\phi}^{SP}\left(2C_6+\frac{1}{2}C_8\right)\right]\right\} \\
&+\cos\theta\left\{-V_{tb}V_{ts}^*\left[f_s F_{B_s\to\phi}^{LL'}\left(a_3+a_4-a_5+\frac{1}{2}a_7-\frac{1}{2}a_9-\frac{1}{2}a_{10}\right)\right.\right. \\
&+M_{B_s\to\phi}^{SP'}\left(C_6-\frac{1}{2}C_8\right)+f_{B_s}F_{ann}^{LL'}\left(a_3+a_4-a_5+\frac{1}{2}a_7-\frac{1}{2}a_9-\frac{1}{2}a_{10}\right) \\
&+M_{ann}^{LL'}\left(C_3+C_4-\frac{1}{2}C_9-\frac{1}{2}C_{10}\right)-f_{B_s}F_{ann}^{SP'}\left(a_6-\frac{1}{2}a_8\right) \\
&\left.\left.-M_{ann}^{LR'}\left(C_5-\frac{1}{2}C_7\right)-M_{ann}^{SP'}\left(C_6-\frac{1}{2}C_8\right)\right]+\left[\eta_s\leftrightarrow\phi\right]\right\}. \qquad (22)
\end{aligned}
$$

$$
\begin{aligned}
A\left(\bar{B}_s^0 \to \eta' \rho^0 \left(\rho^0 \to K^+K^-\right)\right) = & \frac{G_F p_{\bar{B}_s^0} \cdot \sum_{\lambda=0,\pm1} \epsilon(\lambda) g_\rho \epsilon^*(\lambda) \cdot (p_{k^+} - p_{k^-})}{\sqrt{2} s_\rho} \\
& \times \left\{ \frac{\sin\theta}{2} \left\{ -V_{tb}V_{ts}^* \left[f_{B_s} F_{ann}^{LL} \left(\frac{3}{2}a_9 - \frac{3}{2}a_7 \right) + M_{ann}^{LL} \left(\frac{3}{2}C_{10} \right) - M_{ann}^{SP} \left(\frac{3}{2}C_8 \right) \right] \right.\right. \\
& \left. + V_{ub}V_{us}^* \left[f_{B_s} F_{ann}^{LL}(a_2) + M_{ann}^{LL}(C_2) \right] + \left[\rho^0 \leftrightarrow \eta_n\right] \right\} \\
& + \frac{\cos\theta}{\sqrt{2}} \left\{ V_{ub}V_{us}^* \left[f_\rho F_{B_s\to\eta_s}^{LL'}(a_2) + M_{B_s\to\eta_s}^{LL'}(C_2) \right] \right. \\
& \left.\left. - V_{tb}V_{ts}^* \left[f_\rho F_{B_s\to\eta_s}^{LL'} \left(\frac{3}{2}a_7 + \frac{3}{2}a_9 \right) + M_{B_s\to\eta_s}^{LL'} \left(\frac{3}{2}C_{10} \right) - M_{B_s\to\eta_s}^{SP'} \left(\frac{3}{2}C_8 \right) \right] \right\} \right\}. \qquad (23)
\end{aligned}
$$

$$
\begin{aligned}
A\left(\bar{B}_s^0 \to \eta' \omega \left(\omega \to K^+K^-\right)\right) = & \frac{G_F p_{\bar{B}_s^0} \cdot \sum_{\lambda=0,\pm1} \epsilon(\lambda) g_\omega \epsilon^*(\lambda) \cdot (p_{k^+} - p_{k^-})}{\sqrt{2} s_\omega} \times \left\{ \frac{\sin\theta}{2} \left\{ V_{ub}V_{us}^* \left[f_{B_s} F_{ann}^{LL}(a_2) + M_{ann}^{LL}(C_2) \right] \right.\right. \\
& - V_{tb}V_{ts}^* \left[M_{ann}^{LL} \left(2C_4 + \frac{1}{2}C_{10} \right) - M_{ann}^{SP} \left(2C_6 + \frac{1}{2}C_8 \right) \right. \\
& \left.\left. + f_{B_s} F_{ann}^{LL} \left(2a_3 - 2a_5 - \frac{1}{2}a_7 + \frac{1}{2}a_9 \right) \right] + \left[\eta_n \leftrightarrow \omega\right] \right\} \\
& + \frac{\cos\theta}{\sqrt{2}} \left\{ V_{ub}V_{us}^* \left[f_\omega F_{B_s\to\eta_s}^{LL'}(a_2) + M_{B_s\to\eta_s}^{LL'}(C_2) \right] - V_{tb}V_{ts}^* \left[f_\omega F_{B_s\to\eta_s}^{LL'} \left(2a_3 + 2a_5 + \frac{1}{2}a_7 + \frac{1}{2}a_9 \right) \right.\right. \\
& \left.\left. + M_{B_s\to\eta_s}^{LL'} \left(2C_4 + \frac{1}{2}C_{10} \right) - M_{B_s\to\eta_s}^{SP'} \left(2C_6 + \frac{1}{2}C_8 \right) \right] \right\} \right\}. \qquad (24)
\end{aligned}
$$

where the form factor involving η_s is distinguished from η_n by introducing a prime distinction in the upper right corner of F and M with respect to η_s.

B. Input parameters

The V_{tb}, V_{ts}, V_{ub}, V_{us}, V_{td}, and V_{ud} terms in the above equation are derived from the CKM matrix element within the framework of the SM. The CKM matrix, whose elements are determined through experimental observations, can be expressed in terms of the Wolfenstein parameters A, ρ, λ, and η: $V_{tb}V_{ts}^* = \lambda$, $V_{ub}V_{us}^* = A\lambda^4(\rho - \mathrm{i}\eta)$, $V_{ub}V_{ud}^* = A\lambda^3(\rho - \mathrm{i}\eta)\left(1 - \frac{\lambda^2}{2}\right)$, $V_{tb}V_{td}^* = A\lambda^3(1 - \rho + \mathrm{i}\eta)$. The most recent values for the parameters in the CKM matrix are $\lambda = 0.22650 \pm 0.00048$, $A = 0.790^{+0.017}_{-0.012}$, $\bar{\rho} = 0.141^{+0.016}_{-0.017}$, and $\bar{\eta} = 0.357 \pm 0.011$. Here, we define $\bar{\rho} = \rho\left(1 - \frac{\lambda^2}{2}\right)$ and $\bar{\eta} = \eta\left(1 - \frac{\lambda^2}{2}\right)$ [28]. The physical quantities involved in the calculation are presented in the Table 1.

V. ANALYSIS OF DATA RESULTS

A. Direct *CP* violation from the mixing of three vector mesons

Figures 2 and 3 show plots illustrating *CP* violation in the decay processes of $\bar{B}_s \to K^-K^+P$, where we investigate the mixing of $\rho - \omega - \phi$ particles. Figures 2 and 3 depict the variation in A_{CP} as a function of $\sqrt{s}$, which represents the invariant mass of K^+K^-. The central parameter values of the CKM matrix elements are used to obtain these results. The observed *CP* violation in these decay processes provides valuable insights into fundamental physics phenomena, such as vector meson interference.

The maximum *CP* violation from the decay process $\bar{B}_s \to K^+K^-\pi$ in Fig. 2, with a value of −38%, occurs at an invariant mass of 1.02 GeV, which corresponds to the mass position of the ϕ meson. Additionally, small peaks are observed in the invariant mass range $\rho^0 - \omega$. Therefore, it can be concluded that the decay process $\bar{B}_s \to \phi\pi \to K^+K^-\pi$ plays a significant role in this decay channel. Furthermore, for the decay process $\bar{B}_s \to K^+K^-K^0$, a sharp variation in *CP* violation is observed when the invariant masses of K^+K^- pairs fall within the region around 0.75 GeV, reaching a peak value of −70%. In this case, these are the effects from the $\rho^0 - \omega$ mixing mechanism rather than contributions from the QCD penguin dominant decay $\bar{B}_s \to \phi K^0$. Consequently, interference effects are expected to occur within a range 0.7−0.8 GeV. It should be noted that only the tree graph contributes to the $\bar{B}_s \to \phi K^0$ decay. However, the mixed resonance effect between $\phi - \omega - \rho$ leads to a smaller violation peak shift in the invariant mass position

Table 1. Remaining parameters [29, 30] (in units of GeV).

$m_{B_s} = 5.367$	$m_\eta = 0.548$	$f_\phi = 0.23$	$f_k = 0.156$	$f_\omega^T = 0.14$
$m_{K^0} = 0.498$	$m_{\eta'} = 0.958$	$f_\phi^T = 0.22$	$f_\rho = 0.209$	$f_\omega = 0.195$
$m_\phi = 1.019$	$m_{\pi^0} = 0.13498$	$f_\pi = 0.13$	$f_\rho^T = 0.165$	$\Gamma_\rho = 0.15$
$m_\omega = 0.782$	$m_W = 80.385$	$f_n = 0.17$	$f_{B_s} = 0.23$	$\Gamma_\omega = 8.49\times10^{-3}$
$m_\rho = 0.775$	$m_{\pi^\pm} = 0.13957$	$f_s = 0.14$	$C_F = 4/3$	$\Gamma_\phi = 4.23\times10^{-3}$

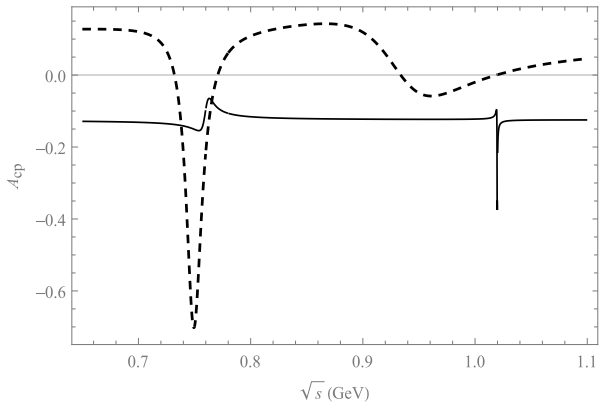

Fig. 2. Plot of A_{CP} as a function of $\sqrt{s}$corresponding to the central parameter values of CKM matrix elements. The solid line (dashed line) corresponds to the decay channel $\bar{B}_s \to K^+K^-\pi(K^0)$.

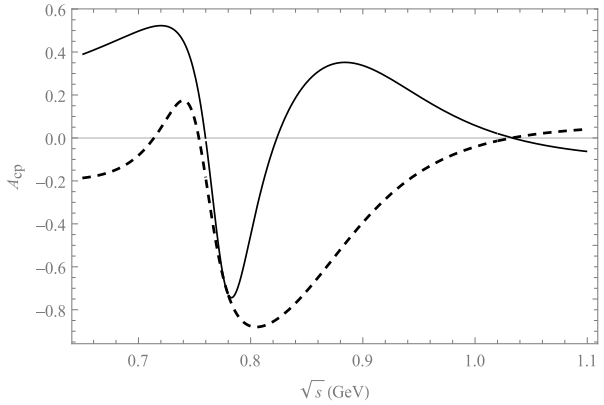

Fig. 3. Plot of A_{CP} as a function of $\sqrt{s}$corresponding to the central parameter values of CKM matrix elements. The solid line (dashed line) corresponds to the decay channel $\bar{B}_s \to K^+K^-\eta(\eta')$.

of the ϕ meson.

Although the decay process $\bar{B}_s \to K^+K^-\eta(\eta')$ is more intricate, we first consider the decay process $\bar{B}_s \to V\eta(\eta')$ involving $\eta(\eta')$. The physical states of η and η' mesons are composed of a mixture of flavor eigenstates, namely, η_n and η_s. Furthermore, there is no contribution from penguin graphs in the decay process $\bar{B}_s \to \phi\eta_s$; hence, the amplitude contribution of the decay $B_s \to K^+K^-\eta(\eta')$ within this entire mixture is negligible. As depicted in Fig. 3, resonant interplay between the large *CP* violation in both invariant mass intervals ($\rho^0-\omega$ and ϕ) ultimately leads to the observed effect shown in Fig. 3. In the figure, it is evident that the *CP* violation peak in $\bar{B}_s \to K^+K^-\eta(\eta')$ occurs with a magnitude of -74% (-88%) near the 0.8 GeV range. This observation allows us to understand the trend of *CP* violation in these decay processes, which is advantageous for our research. Additionally, we can determine the invariant mass value of the K^+K^- pair during significant *CP* violation events, providing an opportunity for experimental measurement.

B. Numerical results of localized integrated *CP* asymmetry

The relationship between *CP* violation and invariant mass in the decay process, as derived in the preceding section, provides valuable insights into the dynamics of *CP* violation. However, to comprehensively investigate regional *CP* violation for future experiments, we perform a local integration analysis of *CP* violation within the studied decay process. Consequently, Table 2 presents the localized *CP* violation for the aforementioned decay processes.

According to Table 2, the integration range (0.98–1.06 GeV) corresponds to the threshold of the $V \to K^+K^-$ decay process. The resonance effect between different particles can lead to more pronounced *CP* violation phenomena in various energy intervals. However, considering the threshold effect for generating K^+K^- meson pairs, we provide the local integral values as shown in Table 2. To compare the similarities and differences between three-particle and two-particle resonance effects, we also present the local integral results of the *CP* violation under two-particle resonance in Table 2.

In the $\bar{B}_s \to K^+K^-\pi^0$ decay process, the value of *CP* violation changes less in the resonance regions above the threshold values owing to any two-particle or three-particle mixing. Although the mixed resonance contributes a peak value of -38% for the $\bar{B}_s^0 \to K^+K^-\pi^0$ decay process in Fig. 2, the local integral values have minimal variation within a specific range in comparison to the overall resonance interval. The values of A_{CP}^Ω exhibit a consistent magnitude of approximately 0.124.

The values of A_{CP}^Ω are small because of contributions from $\phi-\rho-\omega$, $\phi-\rho$, and $\phi-\omega$ mixing. However, a significant *CP* violation of 0.169 can be observed from the

Table 2. Peak local ($0.98\,\text{GeV} \le \sqrt{s} \le 1.06\,\text{GeV}$) integral of A_{CP}^{Ω} from different resonance ranges for the $\bar{B}_s \to K^+K^-\pi(K^0,\eta,\eta')$ decay processes.

Decay channel	$\phi-\rho-\omega$ mixing	$\phi-\rho$ mixing	$\phi-\omega$ mixing	$\rho-\omega$ mixing
$\bar{B}_s \to K^+K^-\pi^0$	-0.124 ± 0.012	-0.126 ± 0.008	-0.147 ± 0.004	-0.124 ± 0.010
$\bar{B}_s \to K^+K^-K^0$	-0.001 ± 0.000	0.0003 ± 0.0001	0.0008 ± 0.0002	0.169 ± 0.004
$\bar{B}_s \to K^+K^-\eta$	0.021 ± 0.0001	0.0174 ± 0.0002	0.010 ± 0.001	-0.237 ± 0.007
$\bar{B}_s \to K^+K^-\eta'$	-0.014 ± 0.005	-0.012 ± 0.008	-0.007 ± 0.002	-0.240 ± 0.005

contribution of $\rho-\omega$ mixing. This behavior changes in the decay process $\bar{B}_s \to K^+K^-K^0$ because it involves the QCD penguin dominant decay $\bar{B}_s \to \phi K^0$ without a tree-level contribution. In this case, only the decay process involving intermediate states with $\rho-\omega$ particles exhibits noticeable *CP* violation.

The decay process $\bar{B}_s \to K^+K^-\eta(\eta')$ is also a special decay process, characterized by the presence of meson mixing between η and η'. The process $\bar{B}_s \to \phi\eta_s$ is a QCD penguin dominant decay without a contribution from a tree diagram, whereas the process $\bar{B}_s \to \phi\eta_n$ involves contributed tree and penguin diagrams. Thus, η_s and η_n mixing results in the presence of a smaller tree contribution for η (η'). Consequently, the involvement of ϕ as an intermediate state in the decay process leads to a reduction in the value of A_{CP}^{Ω}. The *CP* violation induced by the decay process involving $\rho-\omega$ mixing exhibits distinct characteristics, with a maximum value of $-0.237(-0.240)$ observed for the process $\bar{B}_s \to K^+K^-\eta$ ($\bar{B}_s \to K^+K^-\eta'$).

Theoretical errors give rise to uncertainties in the results. In general, the major theoretical uncertainties arise from power corrections beyond the heavy quark limit, necessitating the inclusion of $1/m_b$ power corrections. Unfortunately, there are numerous possible $1/m_b$ power suppressed effects that are typically nonperturbative in nature and therefore not calculable using perturbation theory. Consequently, this scheme introduces additional sources of uncertainty. The first error arises from variations in the CKM parameters, and another is from hadronic parameters, such as the shape parameters, form factors, decay constants, and wave function of B_s mesons. The third error corresponds to selecting appropriate hard scales that characterize the size of next-to-leading order QCD contributions. By employing central values for these parameters, we initially compute numerical results for *CP* violation and subsequently incorporate errors based on the standard deviation in Table 2. We determine that the impact of mixing parameter errors on local *CP* violation is negligible compared to the overall *CP* asymmetry; therefore, this influence value will not be further discussed.

VI. SUMMARY AND CONCLUSION

CP violation in the decay process of the $\bar{B}_s^0$ meson is predicted through an invariant mass analysis of K^+K^- meson pairs within the resonance region, resulting from the mixing of ϕ, ω, and ρ mesons. We observe a sharp change in *CP* violation within the resonance regions of these mesons. Local *CP* violation is quantified by integrating over phase space. For the decay process $\bar{B}_s \to K^+K^-\pi^0$, we find a local *CP* violation value around -0.12 arising from interference between ϕ, ω, and ρ mesons. In decays such as $\bar{B}_s \to K^+K^-K^0$, $\bar{B}_s \to K^+K^-\eta$, and $\bar{B}_s \to K^+K^-\eta'$, *CP* violation is observed owing to contributions from both two-meson and three-meson mixing processes. The local CP violation is large, particularly when involving ρ - ω mixing. Experimental detection of local *CP* violation can be achieved by reconstructing the resonant states of ϕ, ω, and ρ mesons within the resonance regions.

We propose a quasi-two-body approach, namely, $\bar{B}_s^0 \to VP \to K^+K^-P$, to elucidate the three-body decay mechanism of $\bar{B}_s^0 \to K^+K^-P$. During this process, V acts as an intermediate state and undergoes resonance with other particles, ultimately decaying into pairs of K^+K^- mesons. The three-body decay process is appropriately formulated using the quasi-two-body chain decay. We consider the $B \to RP_3$ decay process as a case study for analyzing quasi-two-body decays, where R represents an intermediate resonance state that can further decay into hadrons $P_{1,2}$, and P_3 denotes another final hadron. The process under consideration can be factorized using the narrow width approximation. The expression for $B \to RP_3$ can be written as follows: $\mathcal{B}(B \to RP_3 \to P_1P_2P_3) = \mathcal{B}(B \to RP_3)\mathcal{B}(B \to P_1P2)$, which holds true due to the branching ratio. The effects of the small widths of ϕ, ρ, and ω in quasi-two-body decay processes into KK can be safely neglected. Considering the substantial decay rate of $\rho(770)$, it is reasonable to perform a correction. Using the QCD factorization approach, the correction factor for the decays process $B^- \to \rho(770)\pi^- \to \pi^+\pi^-\pi^-$ is at the 7% level. The parameter η_R is introduced as a quantitative approximation between $\Gamma(B \to RP_3)\mathcal{B}(B \to P_1P_2)$ and $\Gamma(B \to RP_3 \to P_1P_2P_3)$ [31, 32]. When calculating the *CP* violation, this constant can be eliminated, thereby exerting no influence on our ultimate outcome.

Recently, the LHCb experimental group made significant progress in investigating the three-body decay of B mesons and obtained noteworthy findings [33]. By ana-

lyzing previous experimental data, they measured direct *CP* violation in various decay modes such as $B^\pm \to K^+K^-K^\pm$, $B^\pm \to \pi^+\pi^-K^\pm$, $B^\pm \to \pi^+\pi^-\pi^\pm$, and $B^\pm \to K^+K^-\pi^\pm$. Based on the LHCb experiments, future investigations will likely primarily focus on exploring the three-body decays of $\bar{B}_s$.

References

[1] N. Cabibbo, Phys. Rev. Lett. **10**, 531 (1963)
[2] R. Aaij *et al*. (LHCb Collaboration). LHCb-CONF-2012-018(2012)
[3] R. Aaij *et al*. (LHCb Collaboration]. LHCb-CONF-2012-028(2012)
[4] C. Wang *et al*, Eur. Phys. J. C **75**, 536 (2015)
[5] R. Aaij *et al*. (LHCb Collaboration), Phys. Rev. Lett. **111**, 101801 (2013)
[6] Ahmed Aliet *et al*, Phys. Rev. D **76**, 074018 (2007)
[7] Zhen-Jun Xiao, Dong-qin Guo, and Xin-fen Chen, Phys. Rev. D **75**, 014018 (2007)
[8] J. Hua *et al*, Phys. Rev. D **104**, 016025 (2021)
[9] Z. T. Zou *et al*, Eur. Phys. J. C **80**, 517 (2020)
[10] J. P. Lees *et al*. (BaBar), Phys. Rev. Lett. **113**, 201801 (2014)
[11] V.Bertacchi (Belle-Ⅱ), Nucl. Part. Phys. Proc. **324-329**, 107 (2023)
[12] N. E. Adam *et al*. (CLEO), Phys. Rev. Lett. **99**, 041802 (2007)
[13] Y. Nambu, Phys. Rev. **106**, 1366 (1957)
[14] N. M. Kroll *et al*, Phys. Rev. **157**, 1376 (1967)
[15] P.M. IVANOV *et al*, Phys. Lett. B **107**, 297 (1981)
[16] M. N. Achasov *et al*, Phys. Rev. D **94**, 112006 (2016)
[17] Gang Lü *et al*, Chin. Phys. C **46**, 113101 (2022)
[18] Gang Lü *et al*, Eur. Phys. J. C **83**, 345 (2023)
[19] C. E. Wolfe and K. Maltman, Phys. Rev. D **80**, 114024 (2009)
[20] C. E. Wolfe and K. Maltman, Phys. Rev. D **83**, 077301 (2011)
[21] Gang Lü *et al*, Phys. Rev. D **98**, 013004 (2018)
[22] M. N. Achasov et.al., Nucl. Phys. B **569**, 158 (2000)
[23] Y. H. Chen *et al*, Phys. Rev. D **60**, 094014 (1999)
[24] C. Bruch *et al*, Eur. Phys. J. C **39**, 41 (2005)
[25] X. H. Guo *et al*, Phys. Rev. D **63**, 056012 (2001)
[26] Z. H. Zhang *et al*, Phys. Rev. D **87**, 076007 (2013)
[27] Hsiang-nan Li *et al*, Phys. Rev. D **74**, 094020 (2006)
[28] L. Wolfenstein, Phys. Rev. Lett. **51**, 1945 (1983)
[29] R. L. Workman *et al*. (Particle Data Group), Review of Particle Physics, PTEP **2022**, 083C01(2022)
[30] L. Wolfenstein, Phys. Rev. Lett. **13**, 562 (1964)
[31] Hai-Yang Cheng, Cheng-Wei Chiang, and Chun-Khiang Chua, Phys. Rev. D **103**, 036017 (2021)
[32] Hai-Yang Cheng, Cheng-Wei Chiang, and Chun-Khiang Chua, Phys. Lett. B **813**, 136058 (2021)
[33] R. Aaij *et al*. (LHCb), Phys. Rev. D **108**, 012008 (2023)